JOURNAL OF
REINFORCED
PLASTICS &
COMPOSITES

Original Article

*Journal of Reinforced Plastics and Composites*
32(9) 664–678

DOI: 10.1177/0731684412474857
jrp.sagepub.com
SAGE

# Static behavior of three-dimensional integrated core sandwich composites subjected to three-point bending

**Mehmet Karahan[1], Hakan Gul[1], Nevin Karahan[1] and Jan Ivens[2,3]**

**Abstract**

In the current study, the effect of the thickness and the foam density in three-dimensional integrated woven sandwich composites on quasi-static mechanical properties under three-point bending was investigated. Bending modulus and core shear modulus were determined by subjecting the samples, which were cut with varying span lengths according to their core thicknesses, to three-point bending test. Obtained results were optimized by taking core thickness, foam density and panel weights into consideration. Damages that occurred on the tested samples were reported. When compared to conventional foam core sandwich composites, it was found that three-dimensional integrated sandwich composites have superior mechanical properties and due to the fact that the pile yarns in the core and the foam support each other, contrary to conventional sandwich composites no catastrophic core breakage occurs under load, thus the load bearing capacity of the structure is sustained.

**Keywords**

Three-dimensional integrated sandwich composites, three-point bending, damage tolerance

## Introduction

Sandwich composites are used in different areas such as automotive, aerospace, marine and construction industry, and with a wide variety since they combine light weight with high flexural properties.

Three-dimensional (3D) textile production methods have led to interesting developments in the composites industry.[1–3] The use of 3D integrated fabrics in the production of sandwich composites has presented a new concept on this topic.[4–7] 3D integrated sandwich fabrics are made by the velvet carpet weaving technique, where two parallel skins (top and bottom skins) are woven together using pile yarns,[6] keeping a defined distance between the skins to form a core. This integrated connection provides a through-the-thickness reinforcement, in which the pile yarn architecture increases the shear rigidity, which is the most significant disadvantage of many core materials.[8,9] The warp and weft yarns constitute the skins while the pile yarns create a hollow core section, the pile yarn free length determining the core thickness. This sandwich fabric structure has the following advantages: (1) sandwich panels can be produced in a single step, production costs are reduced in line with the shortened production time, (2) top and bottom skins are integrally woven together with the core section and this ensures a stronger binding between the layers: skin-core delamination is virtually impossible and (3) the hollow core section can be filled by several means, thus different functional capabilities can be given to the structure.

There are several studies available on 3D woven sandwich production processes and properties.[10,11] Some researchers examined the mechanical properties

[1]University of Uludag Vocational School of Technical Sciences, Gorukle Bursa Turkey
[2]University of Leuven, Dept. Of Metallurgy and Materials Engineering, Leuven, Belgium
[3]University of Leuven – Thomas More, Department of Engineering Technology, Sint-Katelijne-Waver, Belgium

**Corresponding author:**
Mehmet Karahan, Uludag University, Vocational School of Technical Sciences, Gorukle, Bursa, 16059, Turkey.
Email: mkarahan@uludag.edu.tr

of 3D sandwich composites.[12–15] They found that 3D sandwich composites have a high skin-core delamination resistance and the pile yarns have a significant influence on flatwise compression and shear properties. Shiah et al.[16] examined the elastic modulus and impact properties of 3D integrated sandwich composites. Wang et. al.[17] focused on the three-point bending and flatwise compression properties of multi-face sheet 3D integrated sandwich composites and reported that such structures have superior mechanical properties than mono-spacer 3D sandwich composites. In another study, Wang et al.[18] determined the bending, compression and shear properties of 3D sandwich composites for different foam densities. Brandt et al.[19] examined the planar properties (strength and modulus), damage properties, energy absorption capacities and mechanical breakage properties of different 3D woven composites. Van Vuure et al.[8,20] focused on strength and modulus properties on an empirical and simulative way. 3D sandwich fabrics constitute a good potential for the production of multi-functional composites.[20] Researchers[21–24] also studied other properties of woven textile sandwich composites such as fatigue, damage and low-velocity impact properties: in a study,[25] woven textile sandwich composites were compared with honeycomb sandwiches. The results showed that the properties of 3D woven sandwich composites are better in the weft direction compared to the warp direction.

Compression, bending and impact properties of 3D woven sandwich composites are quite low without any extra skin reinforcement. Also, core shearing resistance decreases as the pile height increases. Due to this, core sections of these materials are generally filled with foam, although it causes a weight increase.[8–12] Change of core thickness and use of foam filling in the core significantly affects the mechanical properties.[7,26,27] Furthermore, core thickness and the use of foam filling require the simultaneous optimization of mechanical properties and weight.

In the present study, 3D sandwich composites with varying core thicknesses were filled with foam of varying densities and the effects of the changes in thickness and foam density on quasi-static mechanical properties were examined. For this purpose, produced samples were subjected to three-point bending tests. Bending modulus and core shear modulus were determined by subjecting the samples, which were cut with varying span lengths according to their core thicknesses, to three-point bending test. The damages in the tested samples are reported.

## Materials and experimental methods

### *3D integrated fabrics*

The 3D sandwich fabrics have been supplied by Parabeam BV (NL). The 3D integrated fabrics used in the research had a core thickness of 10, 15, 18 and 22 mm. All four fabrics are identical in terms of their top and bottom skin layers, the yarns used and the weaving architecture. The only difference is their free pile yarn length and thus the core thickness. Figure 1 illustrates the layout of the yarns in the structure and a typical weaving architecture of a 3D integrated sandwich fabric. It shows that binding yarns connect the top and bottom skins of the structure in thickness direction and consequently the core of the fabric becomes hollow. The parameters of the fabrics used in the study are given in Table 1. All yarns consist of type E-glass fibres. The linear density of the warp, weft and pile yarns is 300 tex.

The structure of 3D integrated sandwich fabrics is different from conventional woven fabrics.[28] Therefore, the fabric geometry was established based on the yarn intersections within the fabrics, to understand the fabric

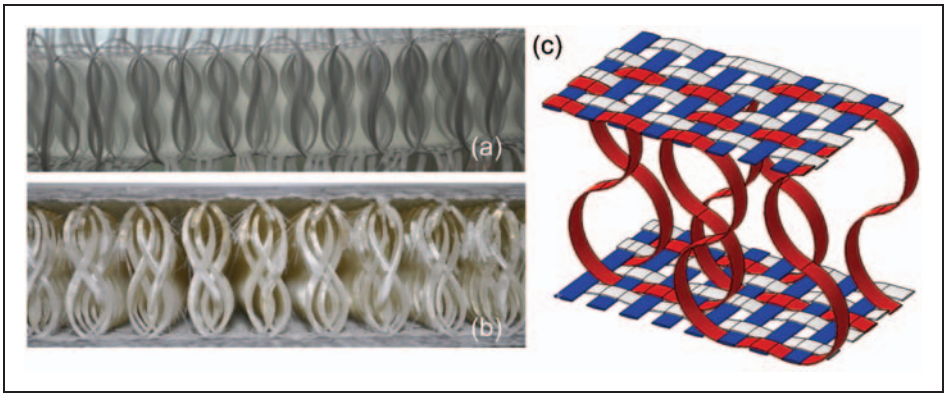


**Figure 1.** Cross-sectional view of 3D dry fabric (a) and resin impregnated plate (b); the schematic display of the 3D fabric structure. 3D: three-dimensional.

**Table 1.** Main properties of the three-dimensional (3D) fabrics and composite plates.

| Core thickness (mm) | 3D dry fabric ($g\,m^{-2}$) | Total dry fabric ($g\,m^{-2}$) | Fibre volume fraction (%) | 3D composite core thickness (mm) | 3D composite plate thickness with additional face sheets (mm) |
|---|---|---|---|---|---|
| 22 | 1680 | 4680 | 36 | 22,1 | 24 |
| 18 | 1720 | 4720 | 36 | 18 | 19.5 |
| 15 | 1600 | 4600 | 36 | 14.9 | 16.3 |
| 10 | 1430 | 4430 | 35 | 10.1 | 12 |

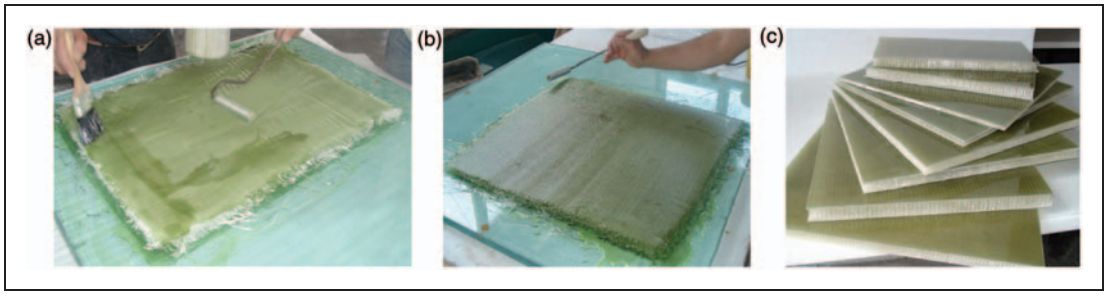


**Figure 2.** Fabrication of 3D integrated panels (a and b) and view of finished plates (c). 3D: three-dimensional.

structure and geometry, and from basic parameters such as yarn width, yarn thickness, weave densities and yarn spacing. The drawings have been carried out with the Katia CAD program. The schematic display of the 3D fabric structure is presented in Figure 1(c).

The top and bottom skins of sandwich panels have been reinforced with an additional plain weave E-glass fabric. Three additional plain woven fabric layers of $500\,g\,m^{-2}$ were used in both the top and bottom skins during composite production.

## *Fabrication of 3D integrated core sandwich panels*

3D integrated sandwich composites were produced from 3D integrated sandwich fabrics. An Atlac 580 AC 300 type vinylester urethane resin was used. A 6% cobalt naphthalate accelerator was added in a ratio of 0.25 phr. A 50% active methyl ethyl kethone peroxide catalyst was used with a mixing ratio of 2 phr. The vinylester resin has a Young's modulus of 3 GPa and 3.4% strain to failure.

All test panels were manufactured using the hand lay-up technique. Production of the panels has been carried out on a glass plate, treated with a release agent. Special care was taken to control the fibre volume fraction during the production of each panel. The top and bottom skins of the panel have been reinforced with an additional three plies plain weave glass fabric. After applying the resin to the skins from both sides, it has been ensured that the resin thoroughly penetrated the entire fabric and that all entrapped air was removed using aluminum impregnation rollers (Figure 2(a) and (b)).

After the application of the resin, the fabrics were kept for 4 h at room temperature for curing. During this time, the impregnated fabric opens up due to the way the pile yarns are woven into the skins. The additional plain weave fabrics have been bonded to the top and bottom skins after the 3D panels have cured with same resin by using hand lay-up. The additional skins cannot be co-laminated as their weight would affect the core thickness. Therefore, the additional fabric layers are laminated onto the sandwich panel after the curing of the 3D sandwich panels. Subsequently, the panels were kept for 1 day for complete curing. The appearances of the plates are shown in Figure 2(c).

The weights of the plates and the weight ratio of fiber and resin of each plate were determined. Since the core sections are hollow, the fiber weight ratios have been determined rather than fiber volume fraction. Table 2 shows the resin and fabric ratios separately for plates of different thicknesses.

## *Foam filling of 3D integrated core sandwich composites*

Some of the panel core sections were filled with rigid polyurethane (PUR) foam, consisting of a mix of $1.08\,g\,cm^{-3}$ polyol and $1.23\,g\,cm^{-3}$ isocyanate (MDI), in a 107/100 isocyanate-polyol mixing ratio (by weight). The foaming process was performed in a mould. During the foam expansion, a pressure of approximately 0.5 bar was built up. A constant temperature

**Table 2.** Finished properties of sandwich samples and their sample codes.

| Core thickness (mm) | Sample code | Foam filling | Density of foam filling ($kg\,m^{-3}$) | Weight ratio of fabric/resin/foam (%) | Unit weight of finished plates ($g\,m^{-3}$) | Weight ratio difference due to foam filling (%) |
|---|---|---|---|---|---|---|
| 10 | A1 | No | – | 64/36/0 | 6710 | – |
| | A2 | Yes | 100 | 57/32/11 | 7550 | 12.5 |
| | A3 | Yes | 120 | 59/27/14 | 7762 | 15.7 |
| | A4 | Yes | 130 | 58/27/15 | 7810 | 16.4 |
| 15 | B1 | No | – | 65/35/0 | 6981 | – |
| | B2 | Yes | 100 | 56/29/15 | 8262 | 18.3 |
| | B3 | Yes | 120 | 54/28/18 | 8532 | 22.2 |
| | B4 | Yes | 130 | 53/27/20 | 8647 | 23.9 |
| 18 | C1 | No | – | 65/35/0 | 7173 | – |
| | C2 | Yes | 100 | 51/27/22 | 8760 | 22.1 |
| | C3 | Yes | 120 | 52/28/20 | 9076 | 26.5 |
| | C4 | Yes | 130 | 50/28/22 | 9218 | 28.5 |
| 22 | D1 | No | – | 64/36/0 | 7088 | – |
| | D2 | Yes | 100 | 51/24/25 | 9283 | 31 |
| | D3 | Yes | 120 | 49/27/24 | 9695 | 36.8 |
| | D4 | Yes | 130 | 49/24/27 | 9839 | 38.8 |


**Figure 3.** Fabrication steps of foam filling process (a and b) and view of foamed and unfoamed panels (c).

of 50°C is maintained throughout the process to enhance the foam penetration between the pile yarns and the homogenity of the foam. The process of injecting foam into the composite plates in the mold is shown in Figure 3. The appearance of the obtained plates with and without foam filling are shown in Figure 3(c). In the end, samples of four different thicknesses (foamed and unfoamed) are obtained. The names of the produced 3D sandwich samples are given in Table 2.

## Experimental studies

*Three-point bending tests.* Three-point bending tests were carried out in accordance with the ASTM C393-62 (standard bending test for flat sandwich constructions) (Figure 4). Three different span lengths were used during the tests. Span lengths were determined separately for each sample according to their core thickness. In the determination of span lengths, the length/core thickness (L/c) ratio was set as 5, 10 and 20 for each sample (Table 3). Bending tests conducted at different span lengths are an alternative method for determining core shear strength and modulus, and it was shown that this method provides results similar to the block shear test.[20] The tests were carried out on samples cut in both weft (0°) and warp (90°) directions. By conducting four tests for each span length, a total of 12 tests were carried out.

The advantages of flexural bending tests are that they are easy to conduct and they allow the determination of the core shear properties of sandwich composites, as well as the in-plane properties of the skin. Three-point bending test geometry provides a combination of bending and shear deformations.

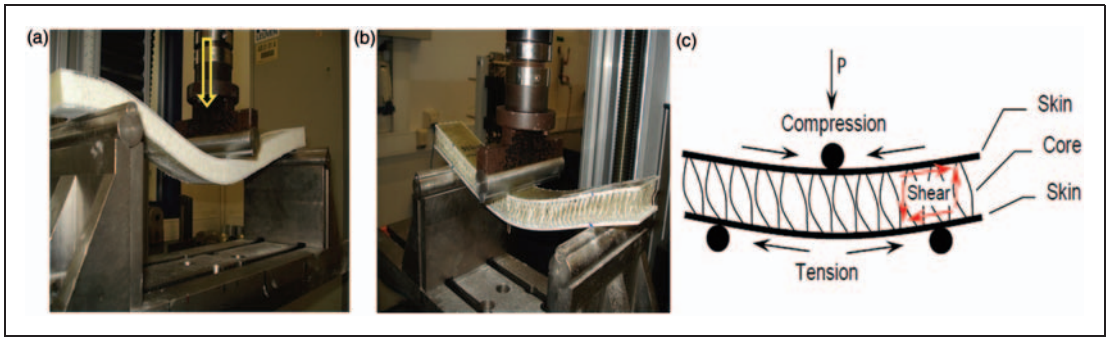


**Figure 4.** View of three-point bending test fixtures (a and b) and schematic display of the stresses that occur on sample core and skins under bending load (c).

**Table 3.** Span lengths of samples used in three-point bending tests.

| Core thickness (mm) | Span lengths for different L/c ratios (mm) | | |
|---|---|---|---|
| | L/c = 5 | L/c = 10 | L/c = 20 |
| 10 | 50 | 100 | 200 |
| 15 | 75 | 150 | 300 |
| 18 | 90 | 180 | 360 |
| 22 | 110 | 220 | 440 |

L/c: length/core thickness.

Elastic analysis of the tests is based on the assumption that shearing completely concentrates on the core material. In this case, vertical deflection $w$ takes place under the $P$ central load and:

$$w = \frac{PL^3}{48D} + \frac{PL}{4N} \quad (1)$$

Here $L$ is the span length while $P$ is the applied load. The bending rigidity $D$ for a symmetrical sandwich structure is given in equation (4). Here, the contribution of core material to the modulus can be ignored. The sandwich shear rigidity $N$ is obtained from equation (5).

$$D = \frac{E_s(h^3 - c^3)b}{12(1 - v^2)} \quad (2)$$

$$N = \frac{G_c(h + c)^2 b}{4c} \quad (3)$$

Here, $E_s$ is the mean skin modulus, $G_c$ is the effective core shear modulus, $h$ is sandwich thickness, $c$ is core thickness, $b$ is sample width and $v$ is the poisson ratio of the skin material.

In order to determine the skin modulus $E_s$ and effective core shear modulus $G$, test results obtained from three different span lengths were used. The total deflection of the sample decreases with increasing span length. Samples are loaded in the elastic region only. Care has to be taken for local deformations at the load introduction and support regions as it may add to the apparent beam compliance.[20] This is particularly true for the cases where shorter spans and a thin skin or weak cores are used.

## Results and discussion

### *Load-displacement curves and damage evaluation*

The span length significantly affects curve characteristics. Load-displacement curves obtained for different span lengths are shown as example in Figure 5 for the samples A1 and A2. A shorter span length results in a higher peak load. The peak load and rigidity are strongly increased by the addition of foam. Sandwich composites behavior under bending depends on the tension/compression resistance of the skins and the shear resistance of the core.

According to the curves shown in Figure 5, in the curve obtained for the lowest span length (L/c = 5), there is a linear elastic part from the start, followed by a non-linear region, and after the peak load, load decreases sharply. This sharp decrease in load corresponds to shear cracks and later the load start to increase again. The next decrease in the peak load at the second peak was caused by skin failure or core-extra skin delamination.

The above-mentioned load-displacement characteristic changes as the span length increases. In the curves obtained for the L/c = 10 ratio, a linear elastic behavior is observed from start until the peak load, followed by a plateau where the load remained nearly constant. This part corresponds to a gradual development of shear damage in the core. At the end of this, part load decreases rapidly. A similar case is also observed for the curves with L/c = 20 ratio, the length of the plateau increases with increasing span-to-thickness ratio.

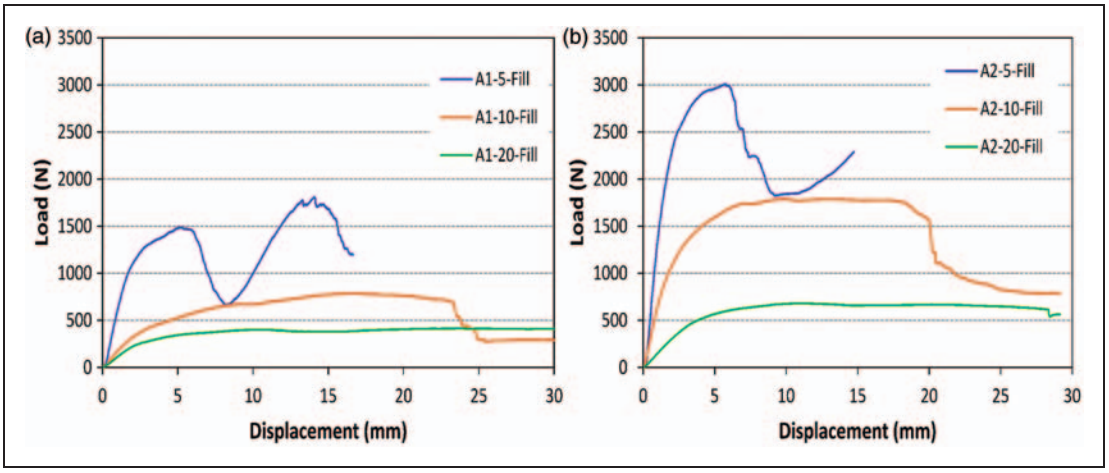


**Figure 5.** Load-displacement curves obtained from three-point bending tests for unfoamed (a) and foamed samples (b) for different span lengths. (A1 and A2 indicate the sample codes; 5, 10 and 20 indicate the L/c ratios for span length; and fill indicate the fill direction tests.) L/c: length/core thickness.

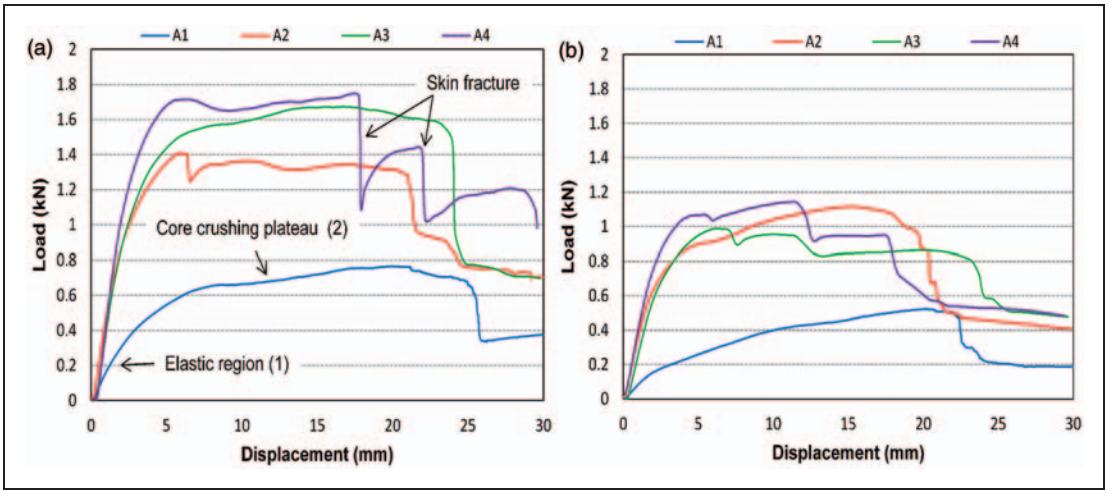


**Figure 6.** Load-displacement curves obtained for L/c = 10 weft (a) and warp (b) directions, based on change of foam density. L/c: length/core thickness.

Figure 6 shows the load-displacement curves for warp and waft directions of sandwich composites under three-point bending load, depending on the foam density. Exemplary load-displacement curves were given only for sample A and L/c = 10. Since the peak load decreases linearly in line with the increase in core thickness, load-displacement curves for other samples are not presented. As it is seen from Figure 6, load-displacement behavior of 3D sandwich composites under bending loading can be generalized as follows: (1) Linear-elastic region, (2) Pile buckling and core shear deformation area and (3) Plastic deformation and extra skin deformation area. In the first region, a linear increase of load was observed. No damage occurs in this part. As for the second area, the decrease of the load indicates the development of damage. The damage is specified as pile buckling and core shear deformation. However, this situation varies according to the core properties of the samples. While the curves of the unfoamed samples, where shear deformation is more dominant, exhibited a long plateau, a shorter plateau is observed for foam filled samples. The third area is where the samples get seriously damaged; core and extra skin rupture or extra skin-core delamination occurred. With shorter span length and increased foam density, skin failure and extra skin-core delamination take place right after the peak load in the upper skin. Furthermore, core and pile yarns subjected to compressive stress showed pile yarn rupture. This was also reported by other researchers.[29,30]

Due to the low shear resistance of unfoamed samples, the load bearing capacity of the skins cannot be

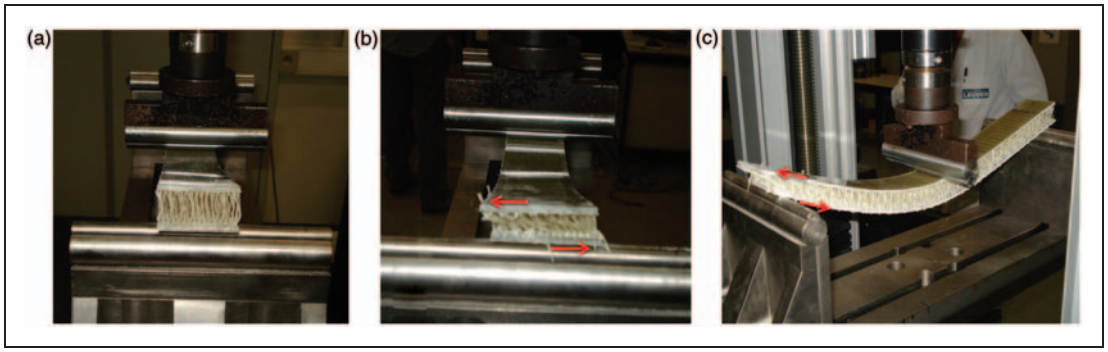


**Figure 7.** Shear deformation taking place in samples without foam filling under bending loading: (a) original state, (b) transversal skin-core shear and (c) longitudinal skin-core shear.

utilized. Shear deformation of unfoamed sandwich material under bending load is given in Figure 7 as an example. This effect increases in line with the increases in span length and core thickness. With the tilting of pile yarns under load, a shear based on core thickness occurs between the upper and lower skins. This part that corresponds to the shearing deformation in the load-displacement curve of unfoamed samples is the plateau where the load remained constant. As the core gets more compressed, both pile yarns and the skins take damage under the bending load and at the end of the plateau the load falls sharply. Comparing the warp and weft directions, it can be seen that the load-displacement curve is nearly the same, yet the peak load in the weft direction is higher. This is due to the fact that the pile yarns in the warp direction exhibit lower bending resistance due to their 8 shape. After the bending loading is removed from the unfoamed samples, the structure has a tendency to turn back to its original form and due to the 8 shape of the pile yarns it exhibits perfect elastic–plastic properties.

From the load-displacement curves of the foam-filled samples, it can be seen that bending stiffness increased considerably. In foam-filled samples, the core shear resistance increases resulting in the dominance of the skin bending rigidity. As foam density increases, higher peak loads are reached. Since the additional skin layers used in all samples were primarily the same, also skin bending rigidity are also expected to be the same. However, due to the fact that the foam contributes to bending resistance, the bending resistance increases with increasing foam density. Bending rigidity in foam-filled samples depends on the foam density and core thickness. As core thickness decreases and foam density increases bending rigidity increases.

The plateau region in the load-displacement curve of foam-filled samples is shorter. This can be attributed to the deformation of the foam. As the foam density increases or as shear resistance rises, the deformation of foam core causes a gradual decrease in the load and no apparent plateau area could be observed. This indicates the advantage of 3D sandwiches over the conventional foam core sandwich composites. In conventional foam core sandwiches, a cracking deformation on the foam core causes a rapid decrease of the load.[31] Whereas, even if a foam core deformation takes place in 3D sandwiches, no rapid decrease in the load occurs because the pile yarns support the foam core and in this way the load-bearing capacity of the structure is sustained.

In a three-point bending test, three different stresses are applied on the sandwich samples. With the loading made from the upper skin of the sample compression stress on pile yarns and torsion and tensile stress on lower sample skins occur.[32–34] (Figure 4(c)). Compression on the piles occurs at load introduction points.[35] The shear stress is maximum in the middle and drops to 0 at the surfaces. Therefore, the shear stress in the skin is neglected. The tensile and compressive stresses are low in the core, because of its low modulus compared to the skin. Shear deformation causes relative displacement of the skins with respect to each other. Therefore the pile yarns are loaded in tension. Deformations on the core and the skins occur with the effect of these three stresses. As the loading continues, a breakage occurs on the interface of extra skins and the core due to the shear stresses. The point of which of these stresses is more effective depends on core thickness, foam density and span length.

Damage that occurs during three-point bending test varies according to span length and the foam filling. Due to this reason, it is necessary to evaluate damage properties separately for samples with and without foam filling. Since shear deformation on the core starts to become dominant as the core thickness increases in unfoamed samples, the damage consists of shear deformation of the pile yarns upper skin breakage. Figure 8 shows the upper skin and side views of the samples without foam filling after bending for $L/c = 10$. No additional skin delamination occurred on the

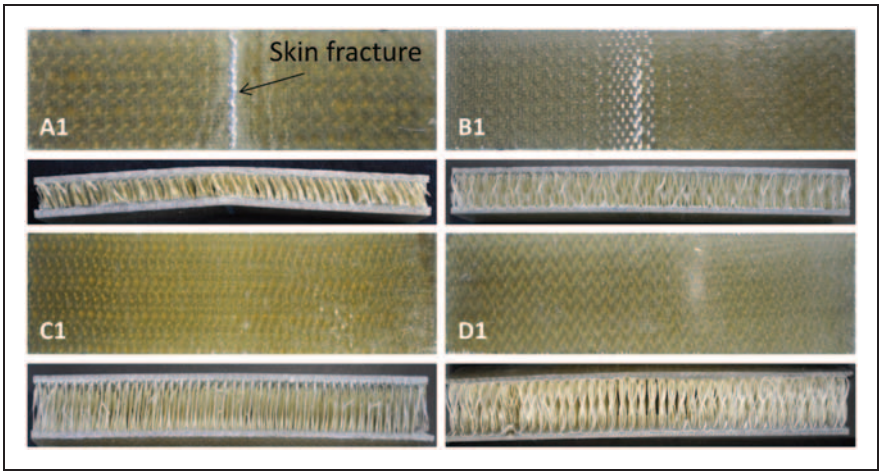


**Figure 8.** Display of the upper skin and side sectional damages for L/c = 10 samples without foam filling. L/c: length/core thickness.

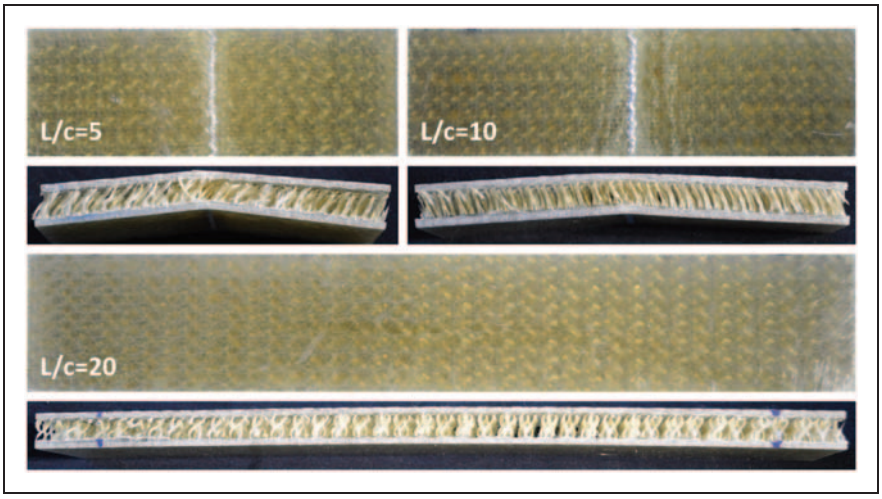


**Figure 9.** Display of upper skin and side sectional damages for A1 sample at varying span lengths.

samples without foam filling. As the core thickness and span length increase, the structure tends more to take its original form when the bending load is lifted. Skin damage does not occur because the core is so weak. Figure 9 shows upper skin and sectional damages for A1 sample at different span lengths.

The damage characteristics in foamed samples change considerably. Since the use of foam increases the shear resistance, the damage that takes place is a mixture of core breakage, skin breakage, extra skin-core delamination and shear deformation (Figure 10). The dominant damage mode changes according to span length, core thickness and foam density. Depending on the increase in core thickness and decrease in foam density, shear deformations can also take place in foam-filled samples. Figure 11 shows shear deformation occurred on foam-filled sample. In such cases, the foam core gets deformed initially at the parts close to the free ends. Upper and lower skin layers slide away from each other with the effect of shear deformation. As core thickness decreases and foam density increases, shear resistance reaches its maximum level and the damages that occur consequently take place in the forms of core breakage, skin breakage or extra skin-core delamination. Shear deformation does not occur as the density of foam filling increases and as loading continues cracking of foam core can be observed (Figure 12). Cracking of the foam core generally starts from the mid section and spreads through the length of the whole sample. Due to the high shear loads in tests with short span lengths, delamination of the extra skin layers takes place. In this case, a sharp load decrease occurs and the load-bearing capacity of the structure is partially maintained. This was also the case even for samples with L/c = 20 span length as the foam density increased (Figure 13). Characteristic of the damages

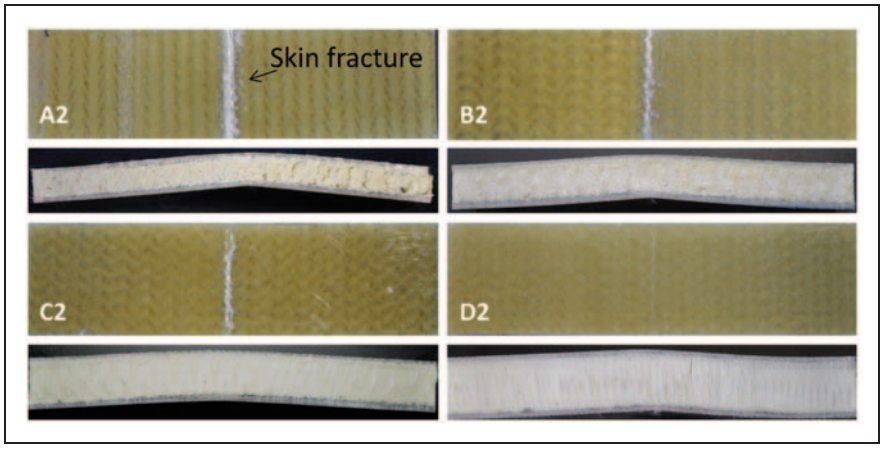


**Figure 10.** Display of the upper skin and side sectional damages for L/c = 10 foam-filled samples. L/c: length/core thickness.

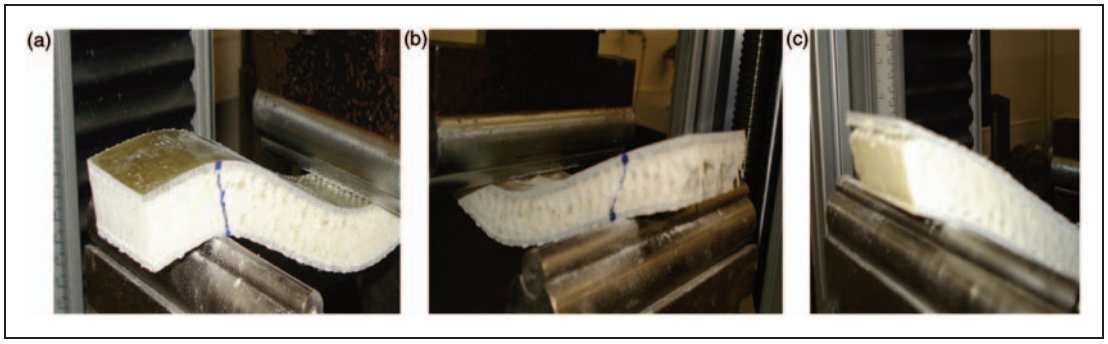


**Figure 11.** View of the shear deformations taking place on foam filled sample (b and c).

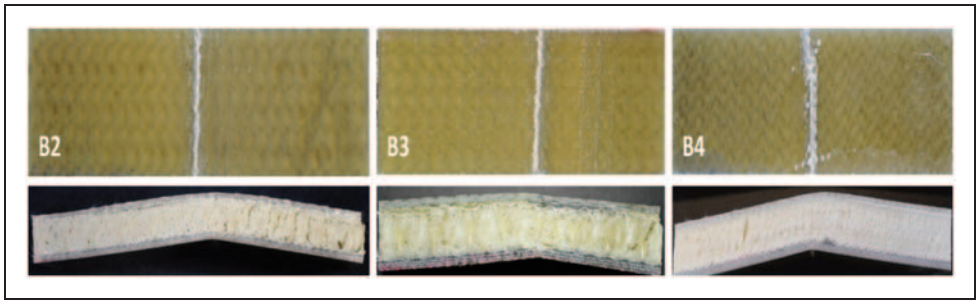


**Figure 12.** Display of damages that occur at different foam densities.

that occurred as the foam density increased did not show a significant difference, yet since less shear deformations took place the damages were usually in the form of skin breakage.

When the damages that occur on 3D integrated composites due to bending load are compared to those on conventional sandwich composites, it can be set forth that the load-bearing capacity of 3D sandwich composites can be sustained. In conventional foam core sandwiches, the foam core breaks near the loading point under bending load and load-bearing capacity of the structure ends[31,36,37] (Figure 14). The important point is that crack in the foam leads to unstable crack growth of this crack and sudden failure. Whereas no such form of damage occurs on 3D sandwiches and the pile yarns in the core and the foam filling support each other during loading. In a 3D sandwich, the pile fibers act as crack stoppers, and that means that there is a more gradual degradation. The damages that occur on the core are only in the form of local foam cracks and

they do not disrupt the integrity of the structure and exhibit that the load bearing capacity of the structure continues. But however the most important problem observed on 3D structures was the delamination of extra skins during loading especially for short span lengths.

## Bending and shear modulus

In the determination of skin and core shear modulus, results of the bending test conducted with three different span lengths were used. In these measurements, while sample width was kept fixed (at 45 mm), sample length was changed according to the thickness of the panel as indicated in Table 3. This method is an alternative to the block shear test method used for determining core shear modulus and previously conducted studies demonstrated that the method is reliable and that there is no significant difference between the results obtained from this method and from the block shear test method.[38]


**Figure 13.** Damages that occur on foam-filled samples for different span lengths (a) and extra skin-core delamination that take place on the samples of L/c = 20 (b and c). L/c: length/core thickness.

Results of skin and core shear modulus are presented in Table 4. The effect of core thickness and foam-filling density on these properties is shown in Figure 15. It is found that the results of shear modulus follow the same trend with the results of bending modulus. Shear modulus increases with the increase of foam density and the decrease of core thickness.

It was determined by comparing the data presented in Table 4 that bending and shear modulus is higher on weft direction when compared to warp direction. As the thickness in samples without foam filling increases from 10 mm to 22 mm, bending modulus decreases from 5800 MPa to 510 MPa and shear modulus decreases from 12.66 MPa to 2.04 MPa for weft direction. On the other hand, in warp direction bending modulus decreases from 2543 MPa to 201 MPa and shear modulus decreases from 8.52 MPa to 1.72 MPa. The decrease in bending modulus during the increase of thickness takes place in accordance with the reduction of core shear resistance, based on the increase in the unsupported length of pile yarns in the core. Highest bending modulus and shear modulus in samples with no foam filling were obtained from the 10 mm sample, the one with the least thickness. On the other hand, bending modulus and shear modulus increased dramatically depending on the addition of foam filling. However, also the weight of the plates increase in line

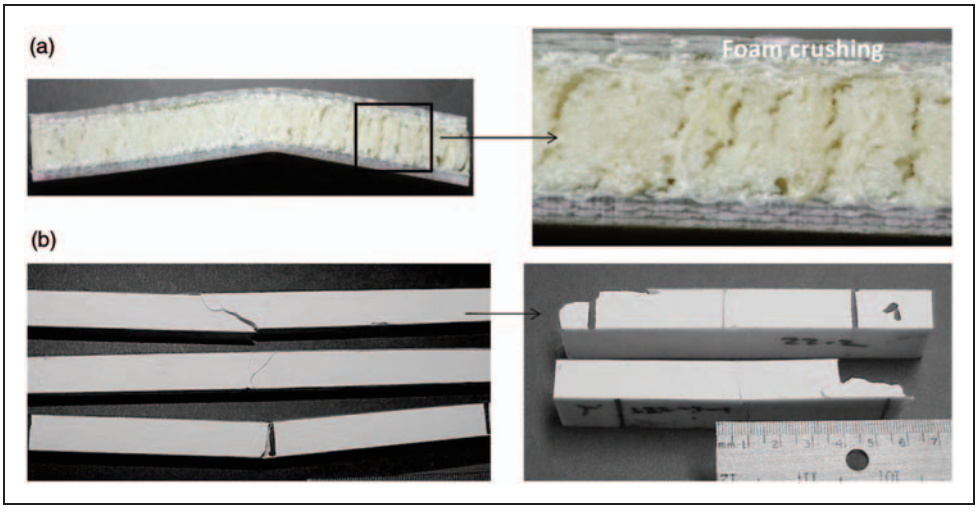


**Figure 14.** Display of the damages due to bending loading in 3D integrated sandwich composites (a) and conventional foam core sandwiches (b).[31] 3D: three-dimensional.

**Table 4.** Three-point bending test results.

| Samples | Test direction | Bending modulus (MPa) | Shear modulus (MPa) | Specific bending modulus (MPa. $m^3 kg^{-1}$) | Specific shear modulus (MPa. $m^3 kg^{-1}$) |
|---|---|---|---|---|---|
| A1 | Fill | 5800 ± 324 | 12.66 ± 0.80 | 864.38 | 1.88 |
| | Warp | 2543 ± 156 | 8.52 ± 0.49 | 378.98 | 1.27 |
| A2 | Fill | 7170 ± 489 | 31.10 ± 1.62 | 925.16 | 4.01 |
| | Warp | 4355 ± 258 | 24.54 ± 1.30 | 561.93 | 3.16 |
| A3 | Fill | 8600 ± 536 | 38.43 ± 1.86 | 1107.96 | 4.95 |
| | Warp | 4921 ± 312 | 30.52 ± 1.55 | 633.98 | 3.93 |
| A4 | Fill | 9278 ± 508 | 40.10 ± 2.13 | 1187.90 | 5.13 |
| | Warp | 5321 ± 216 | 33.05 ± 1.62 | 681.30 | 4.23 |
| B1 | Fill | 2466 ± 128 | 6.19 ± 0.37 | 353.24 | 0.88 |
| | Warp | 1077 ± 34 | 3.92 ± 0.21 | 154.27 | 0.56 |
| B2 | Fill | 4148 ± 185 | 20.54 ± 1.10 | 502.05 | 2.48 |
| | Warp | 2511 ± 96 | 13.94 ± 0.76 | 303.92 | 1.68 |
| B3 | Fill | 5678 ± 304 | 27.95 ± 1.46 | 665.49 | 3.27 |
| | Warp | 2855 ± 164 | 22.71 ± 1.53 | 334.62 | 2.66 |
| B4 | Fill | 5963 ± 276 | 29.01 ± 1.65 | 689.60 | 3.35 |
| | Warp | 3092 ± 153 | 24.4 ± 1.41 | 357.58 | 2.82 |
| C1 | Fill | 788 ± 36 | 2.59 ± 0.16 | 109.85 | 0.36 |
| | Warp | 467 ± 21 | 1.96 ± 0.60 | 65.10 | 0.27 |
| C2 | Fill | 2167 ± 102 | 15.02 ± 1.01 | 247.37 | 1.71 |
| | Warp | 1155 ± 52 | 10.38 ± 0.62 | 131.85 | 1.18 |
| C3 | Fill | 2865 ± 142 | 22.48 ± 1.20 | 315.66 | 2.47 |
| | Warp | 2062 ± 113 | 14.32 ± 0.84 | 227.19 | 1.57 |
| C4 | Fill | 5963 ± 344 | 24.38 ± 1.39 | 330.00 | 2.64 |
| | Warp | 2158 ± 108 | 16.74 ± 1.10 | 234.10 | 1.81 |
| D1 | Fill | 516 ± 23 | 2.04 ± 0.10 | 72.79 | 0.28 |
| | Warp | 201 ± 14 | 1.78 ± 0.50 | 28.35 | 0.25 |
| D2 | Fill | 1870 ± 95 | 12.56 ± 0.90 | 201.44 | 1.35 |
| | Warp | 978 ± 46 | 8.92 ± 0.40 | 105.35 | 0.96 |
| D3 | Fill | 2310 ± 12 | 18.65 ± 1.10 | 238.26 | 1.92 |
| | Warp | 1879 ± 98 | 12.63 ± 1.02 | 193.81 | 1.30 |
| D4 | Fill | 2415 ± 108 | 20.72 ± 1.41 | 245.45 | 2.10 |
| | Warp | 2075 ± 101 | 15.21 ± 1.20 | 210.89 | 1.54 |

with the increase of foam density and it is more meaningful to carry out this evaluation on the basis of the increase in weight.

Compared to the sample without foam filling, in the plate of foamed 10 mm core thickness, specific bending modulus increased by 37% and 79% on weft and warp directions, respectively, while the increase in specific shear modulus on weft and warp directions were 172% and 233%. As for the sample B with 15 mm core thickness, while the increases of specific bending modulus on weft and warp directions were 95% and 131%, the increase in the specific shear modulus on the same directions were 278% and 402%, respectively. For the sample C of 18 mm core thickness, the increases in specific bending modulus on weft and warp directions were 200% and 259%, while the increases in the specific shear modulus on the same directions were 632% and 564%, respectively. For sample D, specific bending modulus increased by 237% and 643% on weft and warp directions, respectively, and specific shear modulus increased by 631% and 515% on the same directions. As the core thickness increased, the effects of the foam filling on the bending modulus and shear modulus of the samples realized on a higher scale. This is primarily due to the excessive decreases of bending resistance and shear resistance that occur as the thickness of samples without foam filling increases.

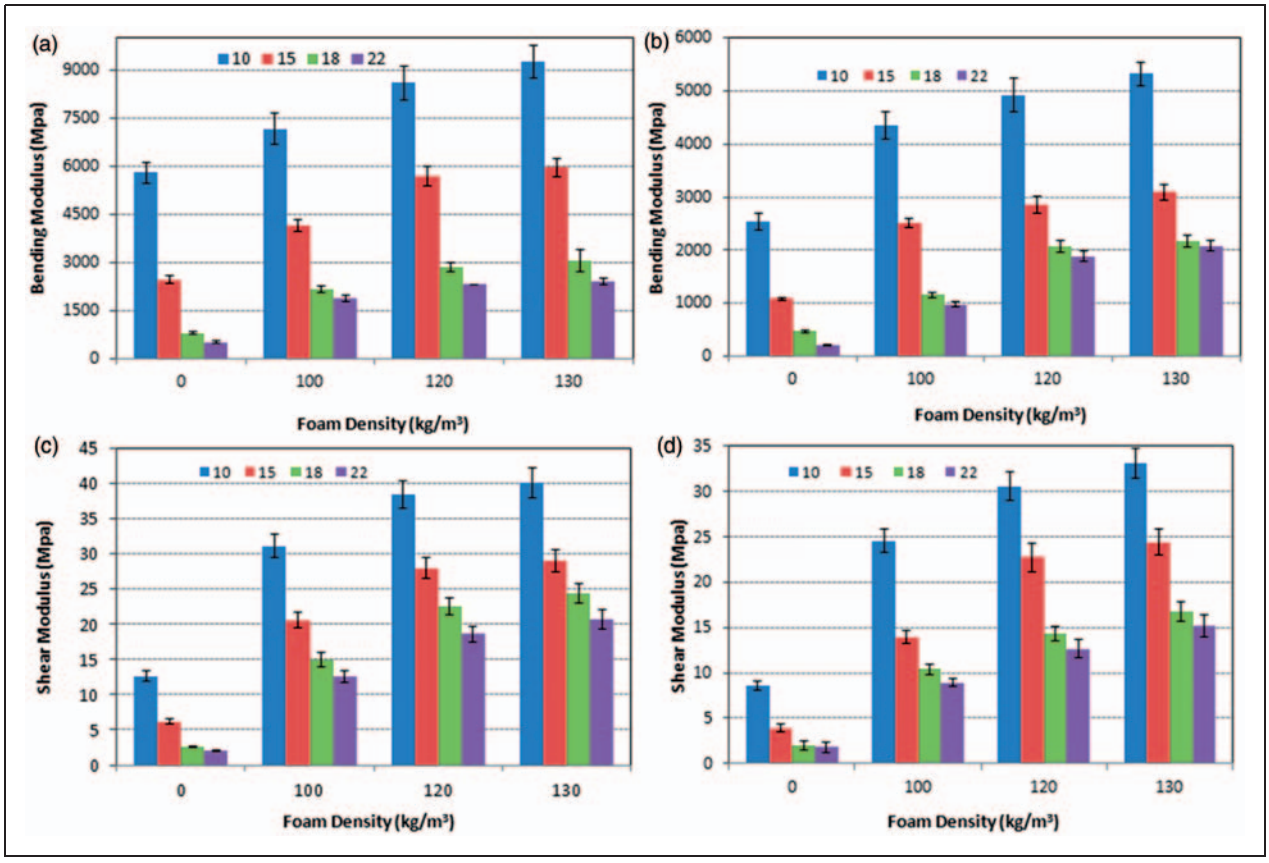


**Figure 15.** Variation of bending and shear moduli on the basis of the changes in foam density: (a and c) for weft direction and (b and d) for warp direction.

According to the three-factor analysis of variance (ANOVA) test conducted at 95% confidence level, it was determined that the test direction (warps and weft direction), foam density and sample thickness have significant effects on bending modulus and shear modulus values. It was also determined that the intersection of these factors also has effects on bending and shear moduli. The same trend was also detected for specific bending and shear moduli.

According to this, the results of each factor, obtained with 95% confidence level according to Student Newman Keuls analysis (SNK), are shown in Table 5. An arrangement of all of the factors according to their respective average values of bending and shear moduli and specific bending and specific shear moduli is presented here. The results of this arrangement can give an idea in terms of optimization of the results.

According to these results, in the evaluation made for all samples bending modulus and shear modulus on weft direction were, respectively, 44% and 25% higher than those on warp direction. As for the assessment made on the basis of unit weight, specific bending and shear moduli on weft direction were, respectively, 46% and 25% higher than those on warp direction. In the assessment made for all samples on the basis of core thickness, when the samples of 10 mm core thickness were compared to those of 15, 18 and 22 mm core thicknesses, respectively, 42%, 63% and 74% higher bending moduli and, respectively, 32%, 50% and 58% higher shear moduli were obtained. In the assessment made for core thickness on the basis of unit weight, the specific bending modulus of the sample of 10 mm core thickness were obtained 47%, 74% and 80% higher than those of the samples of 15, 18 and 22 mm core thicknesses, while the specific shear modulus of the sample of 10 mm were 38%, 58% and 65% higher than that of the compared samples. As for the assessment made for all samples on the basis of core densities, for the samples with densities of 100, 120 and 130 bending modulus values increased by 76%, 125% and 162% in comparison to the sample without foam filling, while the increases in shear modulus were 245%, 372% and 413%. For the assessment made on the basis of unit weight, the specific bending modulus values of samples with densities of 100, 120 and 130 increased by 47%, 84% and 95% in comparison with the sample without foam filling, while the increases in the specific shear modulus values were 283%, 292% and 309%.

**Table 5.** Average bending, shear, specific bending and specific shear moduli values obtained with SNK analysis for different parameters.

| Parameters | Bending modulus (MPa) | Shear modulus (MPa) | Specific bending modulus (MPa. $m^3 kg^{-1}$) | Specific shear modulus (MPa. $m^3 kg^{-1}$) |
|---|---|---|---|---|
| Test direction | | | | |
| Fill | 4249.80 | 20.27 | 502 | 2.42 |
| Warp | 2355.10 | 15.22 | 287 | 1.82 |
| Core thickness (mm) | | | | |
| 10 | 6002.60 | 27.36 | 791 | 3.56 |
| 15 | 3473.70 | 18.58 | 419 | 2.21 |
| 18 | 2202.95 | 13.48 | 207 | 1.49 |
| 22 | 1530.50 | 11.52 | 161 | 1.22 |
| Foam density ($kg\,m^{-3}$) | | | | |
| 0 | 1732.30 | 4.96 | 252 | 0.72 |
| 100 | 3044.04 | 17.12 | 371 | 2.76 |
| 120 | 3896.25 | 23.46 | 463 | 2.82 |
| 130 | 4537.30 | 25.45 | 491 | 2.95 |

The results indicate that decreases in core thickness and increases of foam densities have dramatic effects on bending modulus and shear modulus values.

## Conclusion

In this study, static properties of 3D integrated sandwich woven composites under bending loading were examined in terms of the changes in core thickness and foam-filling density, and the following conclusions were obtained.

- In three-point bending tests, compression stress takes place on the upper skin of sandwich composite, while tensile stress occurs on the bottom skin and shear stress occurs in the core. The dominant stress among these changes on the basis of core shear resistance and this is related with span length, core thickness, use of foam filling and density.
- In the evaluation made after the three-point bending tests carried out on all samples on the basis of unit weight, it was determined that the specific bending and specific shear moduli on waft direction are 46% and 25% higher than those on warp direction.
- In the assessment made for core thickness on the basis of unit weight, the specific bending modulus of the sample of 10 mm core thickness were obtained 47%, 74% and 80% higher than those of the samples of 15, 18 and 22 mm core thicknesses, while the specific shear modulus of the sample of 10 mm were 38%, 58% and 65% higher than that of the compared samples.
- For the assessment made on the basis of unit weight, the specific bending modulus values of samples with densities of 100, 120 and 130 increased by 47%, 84% and 95% in comparison with the sample without foam filling, while the increases in the specific shear modulus values were 283%, 292% and 309%.
- When compared with conventional foam core sandwich composites, 3D sandwich composites have superior mechanical properties and due to the fact that the pile yarns and the foam in the core support each other when under bending load, no catastrophic core breakage takes place, as it does in conventional sandwich composites, and in this way load bearing capacity of the structure continues.

### Funding

This study was funded by Uludag University Scientific Research Unit (UAP-TBMYO/2010-32) and Tubitak (109M350).

### References

1. Lomov SV, Bogdanovich AE, Ivanov DS, et al. A comparative study of tensile properties of non-crimp 3D orthogonal weave and multi-layer plain weave e-glass composites. Part 1: materials, methods and principal results. *Composites A* 2009; 40: 1134–1143.
2. Ivanov DS, Lomov SV, Bogdanovich AE, et al. A comparative study of tensile properties of non-crimp 3D orthogonal weave and multi-layer plain weave e-glass composites. Part 2: Comprehensive experimental results. *Composites A* 2009; 40: 1144–1157.

3. Karahan M, Ulcay Y, Eren R, et al. Investigation into the tensile properties of stitched and unstitched woven aramid/vinyl ester composites. *Text Res J* 2010; 80(10): 880–891.
4. Karahan M, Ulcay Y, Karahan N, et al. Influence of stitching parameters on tensile stregth of aramid/vinyl ester composites. *Mater Sci (Medziagotyra)* 2012 (in press).
5. Barrett DJ. A micromechanical model for the analysis of Z-fiber reinforcement. In: *AIAA/ASCE/ASME/AHS SDM Conference*, Salt Lake City, Utah, 1996, AIAA-96-1329-CP, pp.62–67.
6. ZCL Composites Inc. Company Literature. ST. Edmonton, AB. Canada, 1998.
7. Vaidya UK, Hosur MV, Earl D, et al. Impact response of integrated hollow core sandwich composite panels. *Compos Part A* 2000; 31: 761–772.
8. Van Vuure AW, Pflug J, Ivens J, et al. Modelling the core properties of composite panels based on woven sandwich-fabric preforms. *Compos Sci Technol* 2000; 60: 1263–1276.
9. Judawisastra H, Ivens J and Verpoest I. Determination of core shear properties of 3D woven sandwich composites. *Plast Rubber Compos Process Applicat* 1999; 28: 452–457.
10. Van Vuure AW, Ivens J and Verpoest I. Sandwich panels produced from sandwich-fabric preforms. In: *Proceedings of the International Symposium on Advanced Materials for Lightweight Structures'94*, *ESA_ESTEC*, Noordwijk, Netherlands, 22–25 March 1994, pp.609–612.
11. Van Vuure AW, Ivens J and Verpoest I. Sandwich-fabric panels. In: *Proceedings of the 40th International SAMPE Symposium and Exhibition*. *Anaheim*, *USA*, 1995, pp.966–76.
12. Verpoest I, Wevers M, Ivens J, et al. 3D Fabrics for compression and ımpact resistant composite sandwich structures. In: *Proceedings of the 35th International SAMPE Symposium*, Anaheim, California, 2–5 April 1990, pp.296–305.
13. Zic I, Ansell MP, Newton A, et al. Mechanical properties of composite panels reinforced with ıntegrally woven 3D fabrics. *J Text Inst* 1990; 81(4): 461–479.
14. Karahan M, Karahan N, Gül H, et al. Static behavior of three-dimensional integrated core sandwich composites under compression loading. *J Reinf Plast Compos* 2012 (in press).
15. Bannister MK, Braemar R and Crothers PJ. The mechanical performance of 3D woven sandwich composites. *Compos Struct* 1999; 47: 687–690.
16. Shiah YC, Tseng L, Hsu JC, et al. Experimental characterization of an integrated sandwich composite using 3D woven fabrics as the core material. *J Thermoplast Compos Mater* 2004; 17: 229–243.
17. Wang S, Li M, Zhang Z, et al. Properties of face sheet-reinforced 3-D spacer fabric composites and the integral multi-face sheet structures. *J Reinf Plast Compos* 2010; 29(6): 793–806.
18. Wang B, Wu L, Jin X, et al. Experimental investigation of 3D sandwich structure with core reinforced by composite columns. *Mater Design* 2010; 31: 158–165.
19. Brandt J, Drechsler K and amd Arendts FJ. Mechanical performance of composites based on various three-dimensional woven-fibre performs. *Compos Sci Technol* 1996; 56: 381–386.
20. van Vuure AW, Ivens JA and Verpoest I. Mechanical properties of composite panels based on woven sandwich-fabric performs. *Compos Part A* 2000; 31: 671–680.
21. van Vuurea AW, Verpoest I and Ko FK. Sandwich-fabric panels as spacers in a constrained layer structural damping application. *Composites Part B* 2001; 32: 11–19.
22. Judawisastra H, Ivens J and Verpoest I. The fatigue behavior and damage development of 3D woven sandwich composites. *Compos Struct* 1998; 43: 35–45.
23. Vaidya UK, Hosur MV, Earl D, et al. Impact response of integrated hollow core sandwich composite panels. *Compos Part A* 2000; 31: 761–772.
24. Karahan M, Gul H, Ivens J, et al. Low velocity impact characteristic of 3D integrated core sandwich composites. *Text Res J* 2012; 82(9): 845–862.
25. Zhou GM, Zhong ZS, Zhang LQ, et al. Experimental investigation on mechanical properties of hollow integrated sandwich composites. *J Nanjing Univ Aeronaut Astronaut* 2007; 39: 11–15. [in Chinese].
26. Papa E, Corigliano A and Rizzi E. Mechanical behaviour of a syntactic foam/glass fiber composite sandwich: experimental results. *Struct Eng Mech* 2001; 12(2): 169–188.
27. Bardella L and Genna F. Elastic design of syntactic foamed sandwiches obtained by filling of three-dimensional sandwich-fabric panels. *Int J Solids Struct* 2001; 38(2): 307–333.
28. Karahan M, Lomov SV, Bogdanovich AE, et al. Internal geometry evaluation of non-crimp 3D orthogonal woven carbon fabric composite. *Compos Part A* 2010; 41: 1301–1311.
29. Fan HL, Zhou Q, Yang W, et al. An experiment study on the failure mechanisms of woven textile sandwich panels under quasi-static loading. *Compos Part B* 2010; 41: 686–692.
30. Soares B, Reis L and Silva A. Testing of sandwich structures with cork agglomerate cores. In: Ferreira AJM (ed.) *Proceeding of 8th International Conference of Sandwich Structures (ICSS8)*, Porto, Portugal, 6-8 May 2008, pp.451–462.
31. Gupta N and Woldesenbet E. Characterization of flexural properties of syntactic foam core sandwich composites and effect of density variation. *J Compos Mater* 2005; 39(24): 2197–2212.
32. Russo A and Zuccarello B. Experimental and numerical evaluation of the mechanical behaviour of GFRP sandwich panels. *Compos Struct* 2007; 81: 575–586.
33. Steeves CA and Fleck NA. Collapse mechanism of sandwich beams with composite faces and a foam core, loaded in three-point bending. Part 1: analytical models and minimum weight design. *Int J Mech Sci* 2004; 46(4): 561–583.
34. Vinson JR. *The behaviour of sandwich structures of isotropic and composite materials*. Lancaster, PA: Technomic, 1999.

35. Bekuit JRB, Oguamanam DCD and Damisa O. A quasi-2D finite element formulation for the analysis of sandwich beams. *Finite Element Analysis Design* 2007; 43: 1099–1107.
36. Brooks R, Brown KA, Warrior AN, et al. Predictive modelling of the impact response of thermoplastic composites sandwich structures. In: Ferreira AJM (ed.) *8th International Conference of Sandwich Structures (ICSS8)*, Porto, Portugal, 6–8 May 2008, pp.1157–1168.
37. Lim TS, Lee CS and Lee DG. Failure modes of foam core sandwich beams under static and ımpact loads. *J Compos Mater* 2004; 38(18): 1639–1662.
38. Caprino G and Langel1a A. Study of as three-point bending specimen for shear characterisation of sandwich cores. *J Compos Mater* 2000; 34(9): 791–814.